

A-6865
#3

***Investigation of Pneumatic Inlet and Diffuser Blowing on
a Ducted Fan Propulsor in Static Thrust Operation***

**Technical Final Report
for
NASA Langley Research Center
Hampton, VA**

Contract Number NAG-1-02093

Submitted by:

**Shayne Kondor
Georgia Tech Research Institute
Aerospace, Transportation, and Advanced Systems Lab
7220 Richardson Rd., Smyrna, GA 30080**

March 15, 2003

Title of Investigation

Investigation of Pneumatic Inlet and Diffuser Blowing on a Ducted Fan Propulsor in Static Thrust Operation

NASA Contract Number NAG-1-02093

GTRI Personnel

Shayne Kondor, GTRI Principal Investigator
Aerospace, Transportation & Advanced Systems Lab
Georgia Tech Research Institute
Voice: 770-528-3272
Email: shayne.kondor@gtri.gatech.edu

Robert J. Englar
Aerospace, Transportation & Advanced Systems Lab
Georgia Tech Research Institute
Voice: 770-528-3222
Email: bob.englar@gtri.gatech.edu

Warren J. Lee
Aerospace, Transportation & Advanced Systems Lab
Georgia Tech Research Institute
Voice: 770-528-3469
Email: warren.lee@gtri.gatech.edu

Initiation Year: Year 1: FY 2002

Funding Authorized for Fiscal Year 2002

Grant NAG-1-02093 : \$50,000

Completion Date : December 15, 2003

Status Regarding the Original Objectives: The main objective of this investigation was to determine the effectiveness of Circulation Control as a means to improve off design point operation of a ducted fan. A tip driven turbine model was fabricated by M-Dot Aerospace, and delivered to GTRI in October 2002. The model was subsequently installed in the thrust cell at the MTF Wind Tunnel facility. The fan model was designed similar to a ducted fan tailored for high speed forward flight, and was tested in an off design static lifting condition. Tests were conducted to characterize the baseline performance of the ducted fan, followed by tests to evaluate the effectiveness of using Circulation Control to enhance fan performance in the static lifting condition. This report covers progress on engineering and testing tasks executed under the grant through December, 15 2002.

Section 1. Purpose of Investigation

Tilting ducted fans present a solution for the lifting and forward flight propulsion requirements of VTOL aircraft. However, the geometry of the duct enshrouding the propeller has great a effect on the efficiency of the fan in various flight modes. Shroud geometry controls the velocity and pressure at the face of the fan, while maintaining a finite loading out at the tips of the fan blades. A duct tailored for most efficient generation of static lifting thrust will generally suffer from performance deficiencies in forward flight. The converse is true as well, leaving the designer with a difficult trade affecting the overall performance and sizing of the aircraft.

Ideally, the shroud of a vertical lifting fan features a generous bell mouth inlet promoting acceleration of flow into the face of the fan, and terminating in a converging nozzle at the exit. Flow entering the inlet is accelerated into the fan by the circulation about the shroud, resulting in an overall increase in thrust compared to an open propeller operating under the same conditions¹. The accelerating shroud design is often employed in lifting ducted fans to benefit from the thrust augmentation; however, such shroud designs produce significant drag penalties in axial flight, thus are unsuitable for efficient forward flight applications.

Decelerating, or diffusing, duct designs are employed for higher speed forward flight configurations. The lower circulation on the shroud tends to decelerate the flow into the face of the fan, which is detrimental to static thrust development; however, net thrust is developed on the shroud while the benefits of finite blade loading are retained. With judicious shroud design for intended flight speeds, a net increase in efficiency can be obtained over an open propeller.

In this experiment, conducted under contract to NASA LaRC (contract NAG-1-02093) circulation control is being applied to a mildly diffusing shroud design, intended for improved forward flight performance, to generate circulation in the sense of an accelerating duct design. The intent is to improve static thrust performance of a ducted fan tailored for high speed axial flight, while at the same time significantly reduce the pressure signature on the ground plane. Circulation control on the fan shroud is achieved by the Coanda effect². Figure 1.1 depicts the circulation control scheme at the shroud exit. A highly energized air jet is blown tangent to a curved surface to achieve a localized pressure drop. Sub-ambient static pressure in the jet sheet balances with static pressure in the fan wake, causing the fan discharge near the wall to accelerate around the curved surface.

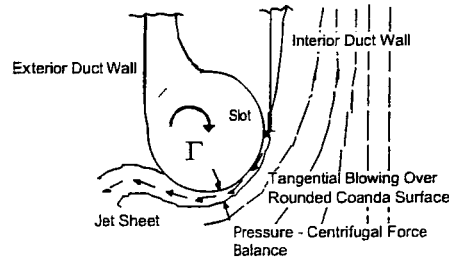


Figure 1.1 Diagram of the Circulation Control Scheme Employed at the Fan Shroud Exhaust Nozzle

Turning the flow around the Coanda surface causes an increase in circulation on the shroud, in the sense of an accelerating shroud.

An additional circulation control device is employed at the leading edge of the shroud inlet. A tangent air jet similar to the exit CC device is injected tangent to the leading edge of the shroud in the direction of the incoming flow. This CC device is intended to help overcome anticipated separation of the flow turning about the sharp leading edge of the shroud. Inlet diffuser stall could be exasperated by application of CC on the exhaust nozzle, if not controlled by this inlet modification.

The effect of applying both CC techniques, separately and in concert was tested on a 5.5" diameter ducted fan model. A crossection view of the fan model is shown in Figure 1.2. The CC technique illustrated in Figure 1.1 was employed at the base exhaust nozzle of the fan. A converging nozzle directs a jet sheet over a radiused surface at the outlet, generating circulation in the sense shown in Figure 1.

Similarly, a CC jet slot is integrated into the leading edge of the shroud inlet. The jet sheet is directed into the inlet and tangent to the inlet surface – generating circulation in the same sense as the exhaust nozzle CC jet.

The fan model was operated in the static thrust regime over a range of fan pressure ratios. CC slot mass flow momentum coefficient (C_{μ}) will be varied from 0 through approximately 0.1, at each fan pressure ratio. The fan was tested in a free jet configuration and normal to a ground plane placed at various distances behind the nozzle. Pressure signatures on the ground plane were recorded in order to determine the effectiveness of the CC application in reducing peak pressure impinging on the ground.

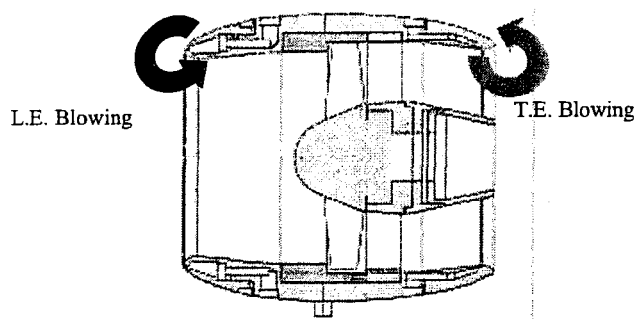


Figure 1.2 Section view of the Ducted Fan Model Showing CC Slot Integration

Section 2. Model and Experimental Set-up

A model ducted fan designed for high speed forward flight designed in conjunction with M-Dot aerospace and constructed by M-Dot Aerospace (Ref. Figure 2.1). During the investigation, the model was operated in a static lifting condition in order to determine the effectiveness of the Circulation Control scheme in enhancing off design operation – as well as reducing the ground pressure signature of the fan wake during VTOL operation.

Employing a GTRI proprietary sizing code, an analysis of the CC slot flow requirements was conducted. Based on previous GTRI internal research³, slot sizings were developed to achieve a range of blowing momentum coefficient $0 < C_{\mu} < 0.25$. Slot opening sizes were provided to M-Dot Aerospace, and independent sizings by M-Dot were reviewed and compared to the GTRI estimates. With sizing estimates in agreement, integration of the CC devices proceeded.

A slot adjustment scheme was developed for the leading edge and exhaust CC jet slots. M-Dot Aerospace developed a set of fixed outer shroud shells with Coanda surfaces of various diameters, surrounding an interior nozzle of fixed diameter. Four shells were constructed with increasing diameters, to provide the following slot heights 0.003, 0.006, 0.009, and 0.012 inches. A sliding adjustable slot arrangement was integrated into the leading edge allowing for adjustment over a range from 0- 0.040”.

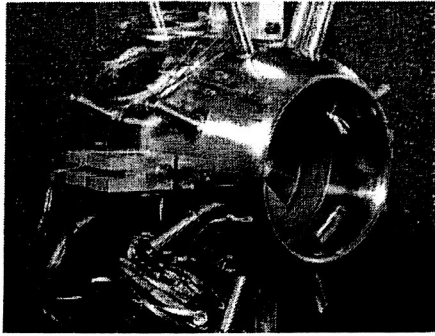


Figure 2.1 Ducted Fan Model

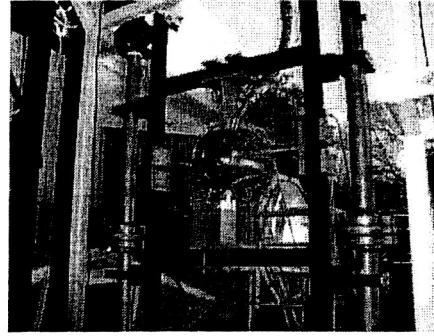
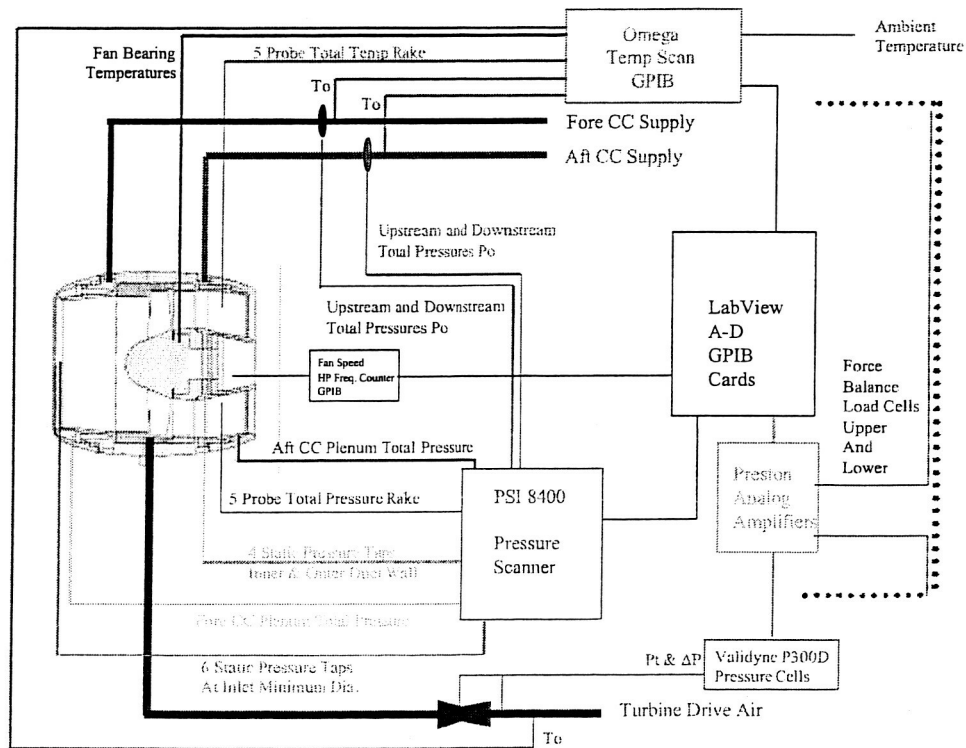


Figure 2.2 Model installation in MTF Thrust Cell

The model was installed in the thrust test cell at the GTRI Model Test Facility. The thrust cell provided a 4 component force balance and multiple pneumatic feed lines to support the test. In addition an ground plane was installed behind the model to investigate operation of the fan in close proximity to the ground.

A diagram of the instrumentation scheme employed is provided in Figure 2.3. A custom LabView VI (script) was written for test control, data collection and on-line data reduction.

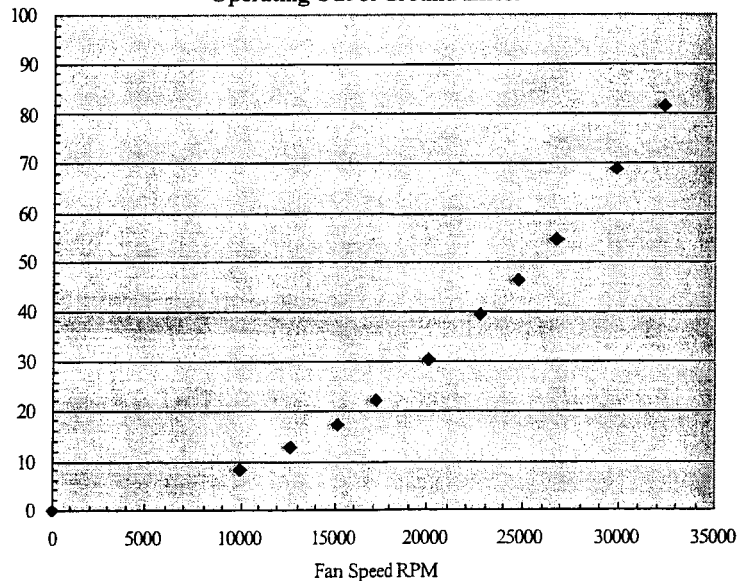


Section 3. Baseline Ducted Fan Performance

Baseline performance of the ducted fan system was established by operating the fan out of ground effect without CC mass flow. Thrust and pressure measurements were taken over sweeps of fan speed to establish performance. Figure 3.1 presents the variation of static thrust with fan speed. Thrust presented is the combination of fan thrust and shroud thrust contributions.

As illustrated by McCormack¹ the thrust generated by a ducted fan is a result of the fan pressure rise and the circulation about the shroud. The fan pressure rise and shroud circulation are interrelated, thus may *not* be measured independently and superimposed.

Figure 3.1
Baseline Ducted Fan Thrust Performance
Operating Out of Ground Effect



Baseline ducted fan pressure ratio is presented as a function of fan speed in Figure 3.2. The pressure ratio was measured by taking a total pressure sample directly behind the fan stators, in the center of the nozzle flow. Pressure ratio was calculated as the ratio of fan exhaust total pressure to freestream total pressure (or ambient pressure in the static thrust case). The center sample was selected as an approximate mean total pressure rise due to the fan alone; due to the high shear present in the nozzle flow it is not clear if the actual fan pressure rise is being measured (ref. Figure 3.3). The irregular total pressure profile downstream of the fan indicates shear due to some degree of mixing in the flow. Shear was expected toward the outermost pressure port due to mixing of the fan flow with the turbine tip drive flow, and the degree of shear increases with tip turbine drive flow (fan speed). However, the irregular total pressure profile warrants additional investigation, as it may affect the performance of the aft CC slot in spreading the fan exhaust jet.

Due to the irregular total pressure profile, the baseline fan pressure ratio (PR) recognized as only an approximation of the pressure ratio due to the shear present in the duct nozzle. Since the measured pressure ratio is approximate, fan speed will be used as to describe the fan operating point.

The baseline duct inlet was determined to be operating in a stalled condition by tuft visualization in the inlet. Despite the inlet separation occurring before the fan, inlet static pressure was nearly uniform

around the inlet (measured at 6 radial locations). The radial variation of inlet static pressure, at the inlet throat, is presented in Figure 3.5. Static pressure drop into the inlet is shown with increasing fan operating speed (or pressure ratio), indicating increasing flow acceleration into the inlet with increasing fan speed. This effect is, of course, expected as thrust of the fan increases with a corresponding increase in mass flow through the fixed inlet geometry. Overall, little inlet distortion is noted when the fan is operating in the baseline configuration (without CC active).

Duct inlet mass flow, turbine drive mass flow, and total mass flow at the ducted fan exit are presented in Figure 3.4. Inlet mass flow was determined using the mean static pressure through the inlet throat. Ideal, isentropic flow through the inlet was assumed; thus, the inlet was treated as a venturi with infinite contraction ratio ($1/\beta$), and $A_{inlet} = 0.14592 \text{ ft}^2$ at the throat:

$$\dot{M} = A_{inlet} \sqrt{2\rho \frac{(P_{\infty} - P_{inlet})}{(1 - \beta^4)}}$$

Turbine drive mass flow required for an operating fan speed correlates with published performance figures for the TDI Model 457 fan unit⁴. Calculated mass flow into the fan inlet is significantly higher than the published mass flow figures for similar operating conditions. This discrepancy can be attributed to two factors:

1. The difference in the fan shroud employed in this test and the inlet configuration used to establish the TDI Model 457 performance.
2. The baseline fan shroud inlet is operating in a stalled condition.

An improved approach to determine inlet mass flow is warranted; possibly a multi-probe total pressure rake positioned in the fan inlet.

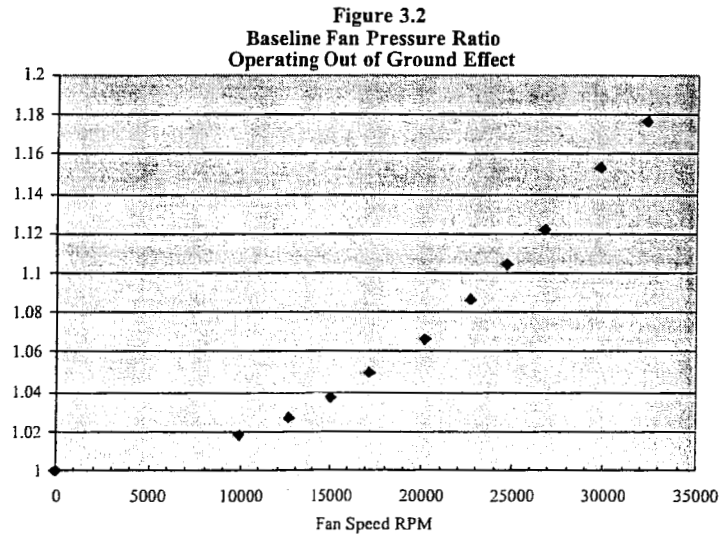


Figure 3.3
Total Pressure Profile Downstream of Fan

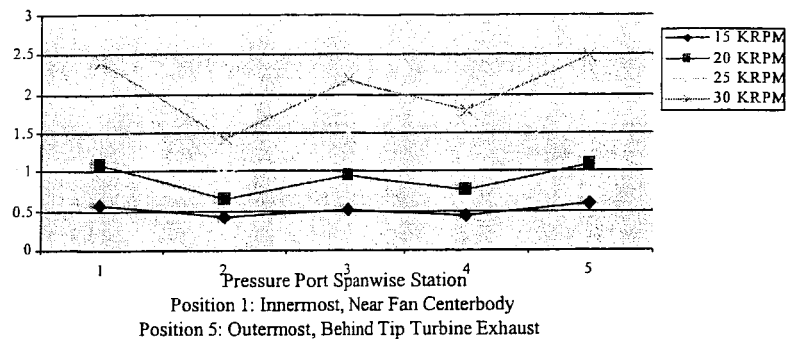


Figure 3.4
Baseline Ducted Fan Weight Flows
Operating Out of Ground Effect

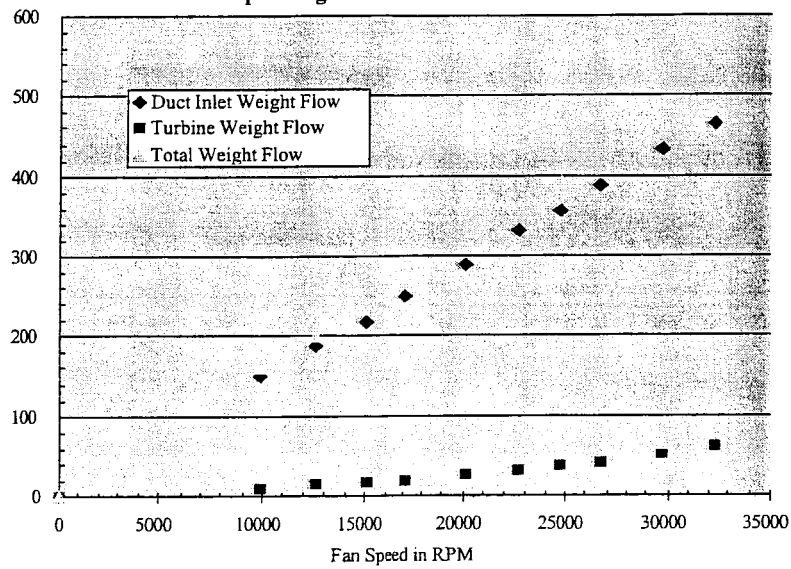
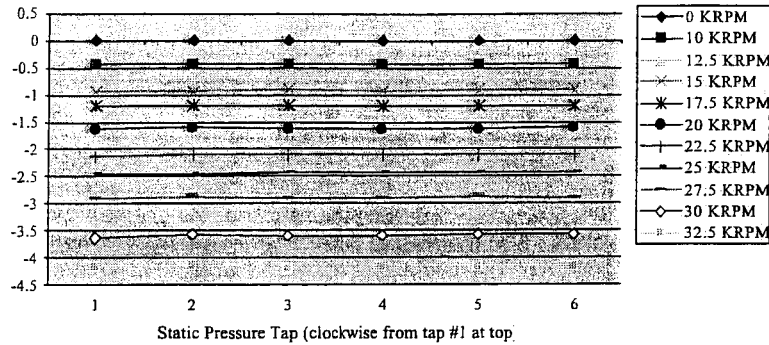


Figure 3.5
Baseline Fan Inlet Static Pressure
Radial Variation Around Inlet Throat
(Operating Out of Ground Effect)



Section 4. Effect of Circulation Control

Circulation Control jets were applied to the fan inlet and exhaust nozzles as described in Section 2. The Aft CC jet slot, at the fan exhaust nozzle outlet, was tested separately and in conjunction with the leading edge CC jet slot at the inlet. In the latter case the leading edge CC slot C_μ is set at the minimum value required to cause the inlet flow to attach (at least over the length of the inlet tufts).

Due to limited testing resources, only a single jet slot configuration was employed for each CC slot. The measured CC slot heights were measured with a feeler gauge as:

Leading Edge CC Slot:	0.020"
Aft (exhaust nozzle) CC Slot	0.005"

Testing of other slot configurations will be deferred to second phase testing.

As noted by Englar (Ref. 4) It is possible for the sharp leading edge slots to deform under stress imparted by pressure in the CC slot plenum and nozzle. Such deformations, if present, were not taken into account in the test series presented.

Fan thrust (T) was non-dimensionalized in the usual manner for propellers (Ref. 2):

$$C_T = \frac{T}{\rho n^2 D^4}$$

While non-dimensional CC jet momentum coefficient was defined in the manner prescribed by Kondor and Heiges (Ref.5) for static thrust applications:

$$C_\mu = \frac{\dot{m} v_{jet}}{T} \quad \text{where} \quad v_{jet} = \sqrt{2 R t_d \left(\frac{\gamma}{\gamma-1} \right) \left[1 - \left(\frac{p_d}{p_\infty} \right)^{\frac{\gamma-1}{\gamma}} \right]}$$

In this definition thrust (T) replaces freestream momentum (qS) in the usual definition (Ref. 3), since zero freestream dynamic pressure would result in an infinite value. V_{jet} is calculated using isentropic expansion to freestream static conditions. For the pressure ratios employed in this test series, the jet nozzle operated from a pure subsonic regime up to an underexpanded operating regime.

The effects on fan performance and inlet mass flow with CC jet slots active are presented in Figures 4.1 and 4.2 respectively. These figures present a free jet case, at a fixed operating point, operating out of ground effect. When only the aft CC slot is active, it is noted that overall thrust is diminished as C_{μ} is increased. At the same time, mass flow into the duct inlet is increased. Based strictly on fan performance, it would be expected to see a thrust increasing with mass flow (at a given operating point). Because the overall thrust decreases, the thrust deficit must result from changes in pressure distribution on the shroud.

Figure 4.1
Thrust Variation with CC @ 25KRPM (PR=1.10)
Operating Out of Ground Effect

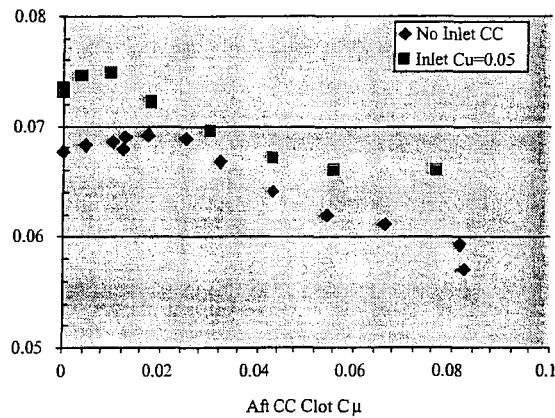
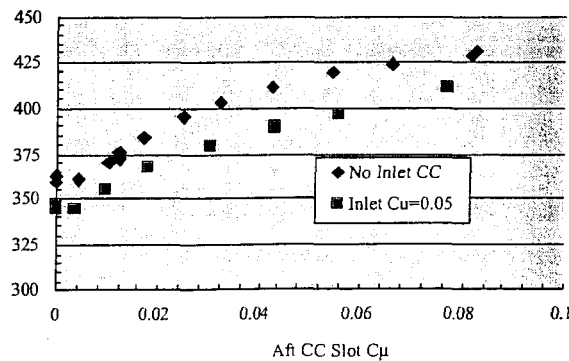


Figure 4.2
Inlet Mass Flow Variation with CC @25KRPM (PR=1.10)
Fan Operating Out of Ground Effect



It is suspected that a strong suction over the trailing edge Coanda surface area is the cause of the thrust deficit. In addition, possible growth of the separation region in the inlet, with aft CC C_{μ} , may also contribute; however, a corresponding loss of inlet mass flow would be expected. It is also plausible that the mass flow measurement at the inlet is adversely affected by a mechanism coupled to the aft CC jet slot flow. At the conclusion of this test series, sufficient data was not available to determine the cause of the thrust deficit noted in the data.

The leading edge CC jet was operated in conjunction with the aft CC jet. In this case the leading edge CC jet was set at the minimum C_{μ} required to attach the inlet flow along the length of the inlet tufts. A tuft visualization in Figure 4.3 (a) shows the inlet separation present when leading edge CC is not employed. Figure 4.3 (b) illustrates the reattachment of inlet flow using minimal leading edge CC blowing.

When the leading edge CC jet slot is operated in conjunction with the aft CC jet slot, some thrust is recovered, while mass flow measurements show a decrease inlet mass flow. The thrust gained may be attributed to two effects:

1. Reattachment of inlet flow, increasing ducted fan operating efficiency
2. Increased leading edge suction around the inlet due to the CC jet.

Again, this mass flow measurement result is counterintuitive, enhanced circulation in the inlet should result in additional mass flow into the duct.

Examining the inlet static pressure distortions in Figure 4.4 & 4.5 sheds some light on a possible cause for the mass flow. In Figure 4.4 it is noted that the inlet throat exhibits little distortion in the radial static pressure profile when the aft CC slot alone is employed. However, in Figure 4.5 it is noted that a significant inlet distortion occurs when the leading edge CC slot is activated. The radial variations in static pressure around the inlet could be caused by uneven jet flow out the leading edge slot, local separation bubbles, or streamwise vorticity shedding from a defect in the jet slot. In any case, variations in inlet static pressures will directly affect the calculated mass flow into the shroud inlet. Checking cases of like aft CC slot C_{μ} clearly a static pressure rise is measured when the leading edge CC slot is activated – resulting in a decrease in calculated mass flow into the inlet. The apparent loss of mass flow when the leading edge CC is an artifact of the apparent cross-talk between the inlet CC jet and the inlet static pressure taps.

It is difficult to establish the actual flow into the inlet due to the cross-talk with the inlet CC jet. Additional instrumentation is needed to accurately determine the inlet mass flow when the inlet CC jet is active. Likewise additional investigation of the flow near the inlet leading edge is warranted.

The only significant effect which may be definitely attributed to the inlet CC jet is reattachment of separated inlet flow. Reattachment of the inlet flow does result in a significant enhancement in static thrust performance of the fan over the baseline performance at the same operating condition.

Figure 4.3 Tuft Visualization of Inlet Condition

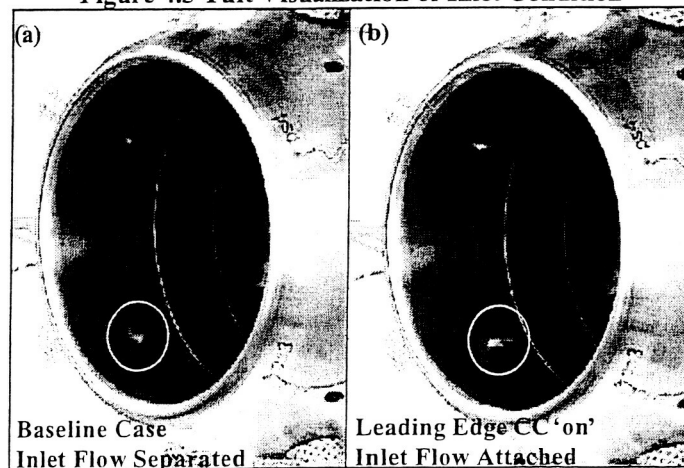


Figure 4.4
Inlet Static Pressure Variation with Aft CC

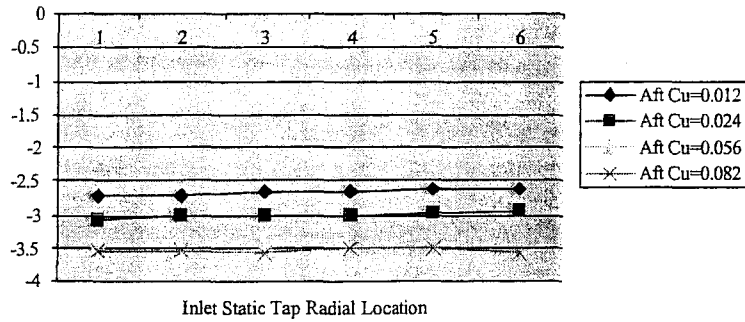
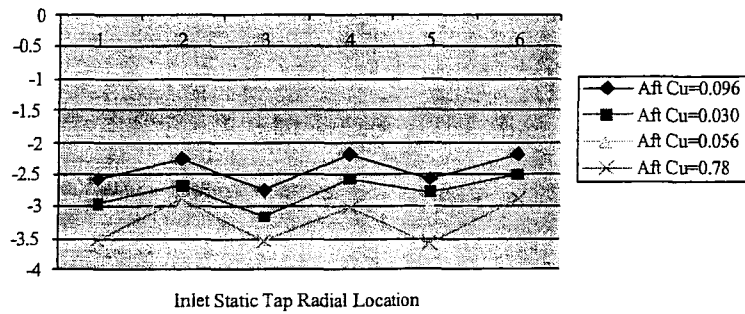


Figure 4.5
Inlet Static Pressure Variation with Simultaneous Inlet and Aft CC



Section 5. Operation in Proximity to a Ground Plane

A primary objective of this study is to assess the effectiveness of CC in reducing the pressure signature of the ducted fan wake impinging on the ground. To simulate operation in proximity to a ground plane, a representative ground plane was positioned at several stations behind the model and pressure signatures of the impinging wake were measured. A 1-D array of 18 static pressure taps were oriented from the center of the ground plane radiating outward in an even 1 inch spacing. This arrangement provided a pressure signature from the center of the impinging wake out to greater than 6 fan exit diameters.

Ground plane static pressure was non-dimensionalized against freestream static pressure (p_∞):

$$C_p = \frac{P_s}{P_\infty}$$

Fan thrust (T) was non-dimensionalized in the manner prescribed in Section 4.

In order to relate the overall aerodynamic force of the impinging wake on the ground plane, the incremental pressures were integrated along the pressure tap array:

$$\int C_p d\left(\frac{y}{r}\right) \text{ where } \frac{y}{r} \text{ is the non-dimensional radial station.}$$

Figures 5.1, 5.2, 5.3, and 5.4 relate the pressure signature with increasing aft CC C_μ for a single operating condition of 25KRPM ($\sim PR=1.10$). Ground plane pressure profiles are shown for non-dimensional heights of 1.5, 3, 6, and 10 nozzle exit diameters above the ground plane. It is noted that increasing C_μ generally results in a decrease in peak pressure on the ground plane; the effect is greater as the fan is situated at greater distances from the ground plane.

In close proximity to the ground plane (Fig. 5.1 & 5.2) a slight dent in the pressure profile is noted near the centerline; this dent may be due to flow separation off the fan centerbody base. In these cases a pressure peak is noted as C_μ is increase; the peak occurs after the dent disappears – indicating some degree of flow reattachment around the centerbody base. Referring to Figure 5.5 it is noted that the overall aerodynamic load on the ground plane generally decreases with increasing C_μ .

As the fan is moved to greater height above the ground plane, in Figures 5.3 & 5.4, no increase in ground plane pressure is noted with increasing C_μ . On the contrary, the effect on the overall aerodynamic load on the ground plane is more far pronounced with increased height; the integrated aerodynamic load in Figure 5.5 decreases dramatically with increasing aft CC C_μ . In the most extreme case, at a height of 10, the peak pressure is diminished by 7 fold with a CC jet momentum of only 7-8% of the fan wake. In this case the pressure static pressure rise at the ground plane is only 10% of ambient. The enhanced effectiveness in diminishing peak ground pressure with height over the ground plane is expected with the natural jet breakup mechanisms occurring several diameters downstream of the exit.

For this test series C_μ values were limited to the range shown to be most effective at affecting a fan flow in previous study³. It is anticipated that extension of C_μ values beyond 0.08 may yield more dramatic effects. In a tuft visualization study at higher C_μ values, dramatically enhanced free jet spreading was noted; this may extrapolate to the impinging jet case.

Figure 5.1
Ground Plane C_p at $H=1.5$ Dia.
for Nominal Fan Speed 25000 RPM \pm 3%
Aft CC Slot C_μ in Legend

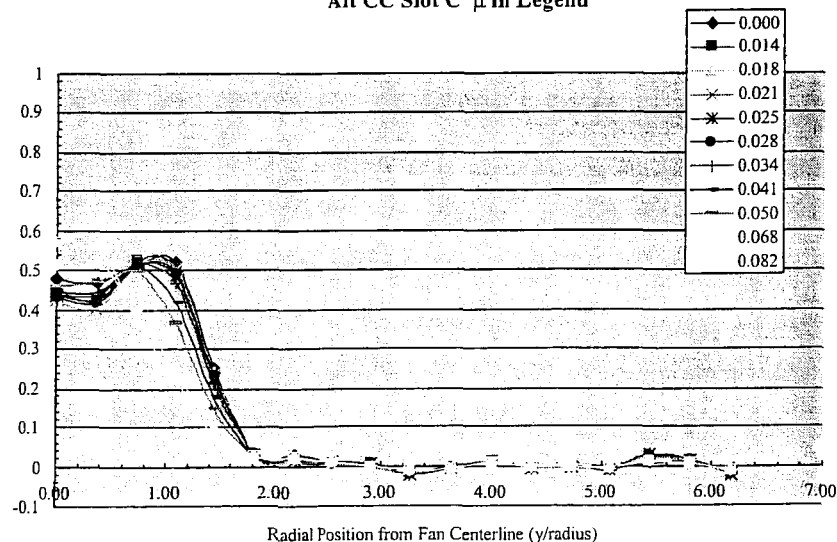


Figure 5.2
Ground Plane C_p' at H=3.0 Dia.
for Nominal Fan Speed 25000 RPM \pm 3%
Aft CC Slot C_μ in Legend

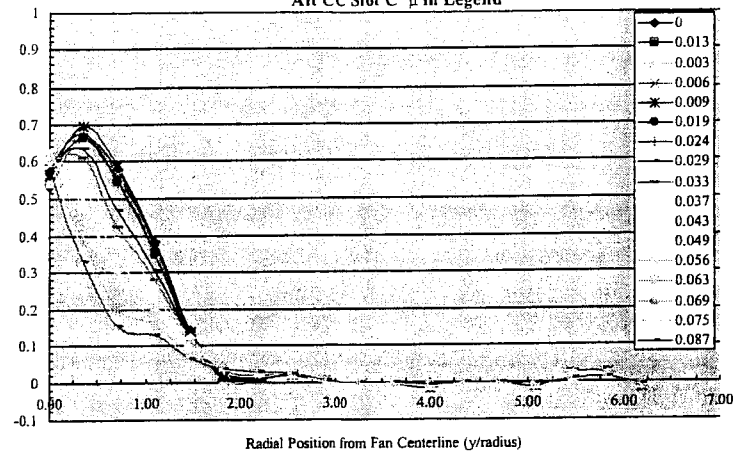


Figure 5.3
Ground Plane C_p' at H=6.0 Dia.
for Nominal Fan Speed 25000 RPM \pm 3%
Aft CC Slot C_μ in Legend

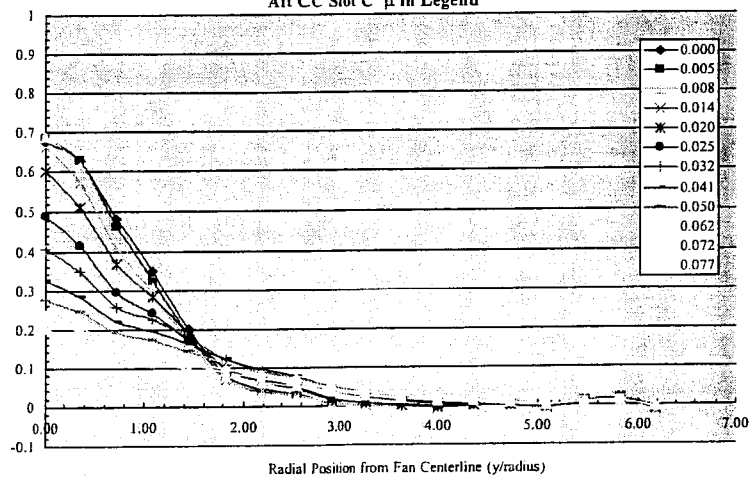


Figure 5.4
Ground Plane C_p at $H=10.0$ Dia.
for Nominal Fan Speed 25000 RPM $\pm 3\%$
Aft CC Slot C_μ in Legend

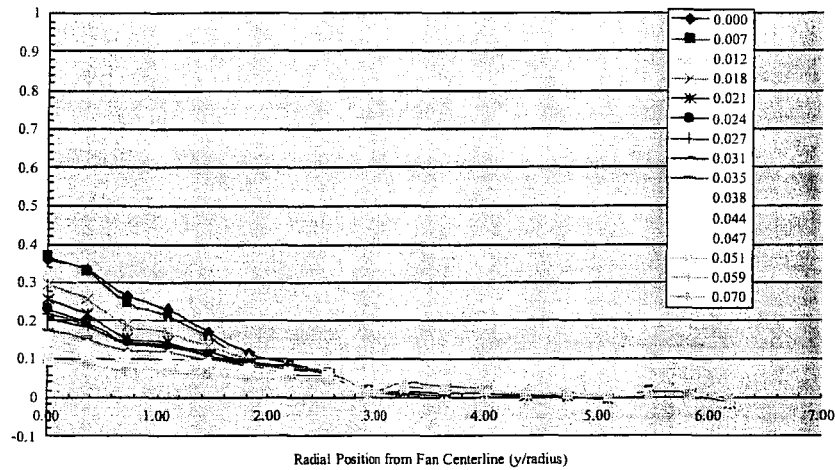
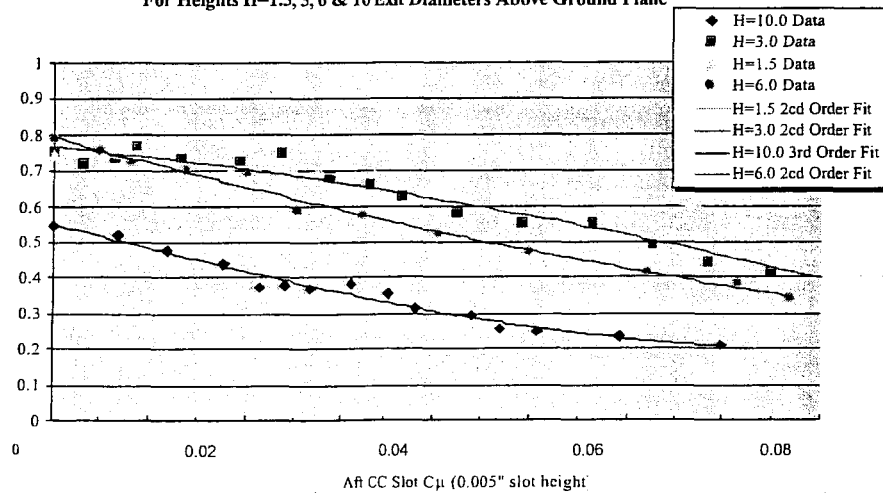


Figure 5.5
Integrated Aero Load on Ground Plane @ 25K RPM $\pm 3\%$
For Heights $H=1.5, 3, 6$ & 10 Exit Diameters Above Ground Plane



Section 6. Flow Visualization

Flow visualization was performed to illustrate and explore the fan wake spreading affected by aft CC jet slot blowing. Obtaining meaningful flow visualization proved far more challenging than anticipated in the proposal stage. Attempts to oil seed the flow through the fan were unsuccessful as the fan wake tended to disperse the oil droplets to a point where imaging was not possible. In addition, even seeding of the flow through the inlet proved extremely difficult.

Tuft visualization was employed as a fallback means of obtaining visualization of the flow behind the fan. Icing conditions at higher pressure ratios also provided a natural means of flow visualization with condensation in the flow providing some degree of visualization. Figures 6 (a), (b), & (c) present a case of free jet wake at a fan pressure ratio of 1.12 and three aft CC conditions; tuft strip spacing is approximately 0.75 dia.

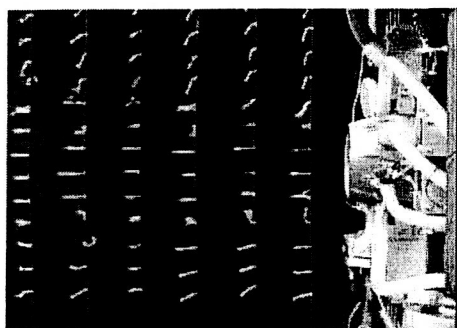


Figure 6(a)

Tuft Visualization with no Aft CC
27.5KRPM (PR=1.12)

Tight jet core with mixing occurring
far downstream of the nozzle..

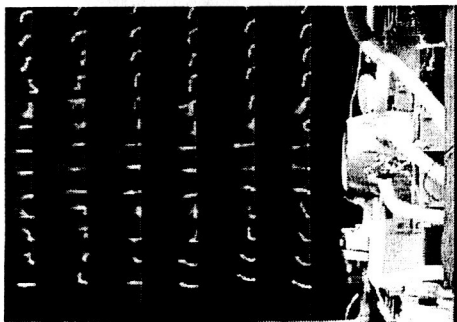


Figure 6(b)

Tuft Visualization with Aft CC
 $C^* < 0.1$, 27.5KRPM (PR=1.12)

Enhanced jet spreading is noted along
with enhanced mixing downstream.

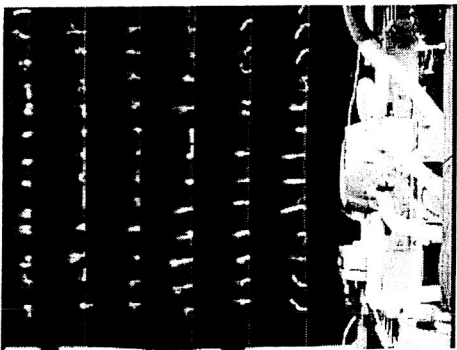


Figure 6(c)

Tuft Visualization with Aft CC,
 $C_m > 0.10$, 27.5KRPM (PR=1.12)

Greatly enhanced jet spreading rate,
Extreme mixing noted beyond 1.5 dia.
Downstream of the nozzle.

Section 7. Conclusions

The ability to affect the wake ducted fan by application of Circulation Control on the shroud has been demonstrated. The application of circulation control, via a Coanda surface and tangent jet slot built into the shroud nozzle, has shown some effectiveness at spreading the fan wake and modifying ground pressure signatures. Likewise, a Coanda surface and tangent jet slot built into the inlet of the shroud has proven effective in reattaching separated flow within the inlet. An unanticipated drawback of the nozzle (aft) CC device was the significant thrust penalty incurred; however, the thrust penalty could be – at least partially – offset by the suction on the inlet affected by the inlet CC device.

Due to some limitations of the current instrumentation set-up and scope of the effort, conclusions on the exact flow mechanisms governing the observed phenomena can not be made. In addition, the full scope of the feasible design space for incorporation of circulation control on a fan shroud has not been explored; the dearth of existing data is not adequate for design purposes. It is recommended that further study be given to the concept, including exploration of variations on Coanda surface and jet slot design variables. The following recommendations are made:

1. Detailed exploration of fan wake flow field using PIV and hot wire surveys.
2. Retrofit of the model inlet with a multi-probe total pressure rake.
3. Exploration of CC effectiveness at C_{μ} values > 1 .
4. Continued investigation testing with variations of CC jet slot heights (inlet & nozzle)
5. Continued investigation with exhaust nozzle coanda surfaces having less than 90° turning angle.

Other means of flow control, both passive and active, should be compared to CC on the basis of effectiveness in spreading the fan exhaust. Methods such as nozzle taps, swirl injection, and normal mass injection into the jet layer could prove effective in achieving similar results.

References

1. McCormick, B., Aerodynamics of V/STOL Flight, Academic Press 1967.
2. Englar, R. J., "Circulation Control Pneumatic Aerodynamics: Blown Force and Moment Augmentation and Modification; Past, Present & Future," AIAA Paper 2000-2541.
3. Kondor, S., Heiges, M., "Active Flow Control for Control of Ducted Rotor Systems", AIAA Paper 2001-0117.
4. TDI Model 457 Fan Manual, Tech Development Inc.